ELSEVIER

Polymer 42 (2001) 1697–1705

polymer

www.elsevier.nl/locate/polymer

Influence of annealing on the microstructural, tensile and fracture properties of polypropylene films

D. Ferrer-Balas, M.Ll. Maspoch*, A.B. Martinez, O.O. Santana

Departament Ciència dels Materials i Enginyeria Metal-lúrgica, Universitat Politècnica de Catalunya, Av. Diagonal 647, 08028 Barcelona, Spain

Received 21 February 2000; received in revised form 15 May 2000; accepted 13 June 2000

Abstract

The influence of annealing temperature on the fracture properties of iPP films (one homopolymer and two propylene–ethylene block copolymers) is presented. The fracture behaviour is studied by means of the Essential Work of Fracture (EWF) procedure, and is complemented by the study of the effect of thermal treatment on tensile properties and microstructure, using differential scanning calorimetry (DSC) and wide-angle X-ray scattering (WAXS). It is shown that the initial metastable phase of quenched iPP films, widely known as smectic, transforms gradually into the monoclinic form as the annealing temperature is increased, resulting in an important improvement of the tensile properties, whereas the fracture parameters have different evolutions depending on the ethylene content. The reasons for a decrease in the essential work term and an increase in the plastic term as the crystal perfection grows are discussed on the basis of the microstructural changes of the crystalline phase and the smectic–monoclinic strain-induced phase transformation.

Keywords: Polypropylene; Annealing; Essential work of fracture

1. Introduction

Recently, various papers have treated the influence of thermal treatment of iPP films on their mechanical and fatigue life properties [1–3]. In addition, it has been shown that annealing isotactic polypropylene (iPP) homopolymer and copolymer pieces can improve notably their toughness [4–6], although no studies on films of iPP have been done concerning this matter, probably because until now it was difficult to find a reliable method for studying fracture parameters for thin ductile films. However, the recent development of the Essential Work of Fracture (EWF) procedure as a good alternative for studying polymeric films with a fracture mechanics approach [7–10] gives the opportunity of analysing the effect of annealing on film toughness, and thus increasing the understanding of the relationship between morphology and fracture properties in semicrystalline polymers. Moreover, this work contributes to estimate the EWF procedure possibilities, which in recent years is being used in a wide range of studies.

The material studied is particularly interesting because it suffers a phase transformation with annealing that modifies substantially its microstructure. Initially, when an iPP film is cast-extruded and rapidly cooled to room temperature, a metastable phase is obtained, giving an intermediate state between ordered and amorphous phase, and widely known as "quenched" or "smectic" phase (*sm*-PP) [1,12,13]. This phase is stable at room temperature, but transforms into the monoclinic iPP phase (α-PP) on heating to temperatures above 70–80°C [13,14], or by applying plastic deformation to the material [2].

The EWF concept, which has been increasingly used in recent works, was developed initially by Cotterell and Reddel [15] on the basis of Broberg's idea [16], who suggested that the total work of fracture (W_f) dissipated on a pre-cracked body could be divided into the work done in two distinct zones, the inner and the outer regions, yielding to the essential work of fracture (W_e) and the non-essential (or plastic) work of fracture (W_p), respectively (Fig. 1). The former corresponds to the instability in the crack tip — the real fracture process region — and the latter to the yielding in the surrounding region. Thus, the following relation can be written:

$$W_f = W_e + W_p = w_e lt + w_p \beta l^2 t \quad (1)$$

where w_e is the specific essential work of fracture (per ligament area unit), w_p is the specific non-essential work of fracture (per volume unit), l is the ligament length, t is the

* Corresponding author. Fax: +34-934-016-706.
E-mail address: maspoch@cmem.upc.es (M.L. Maspoch).

0032-3861/01/$ - see front matter
PII: S0032-3861(00)00487-0

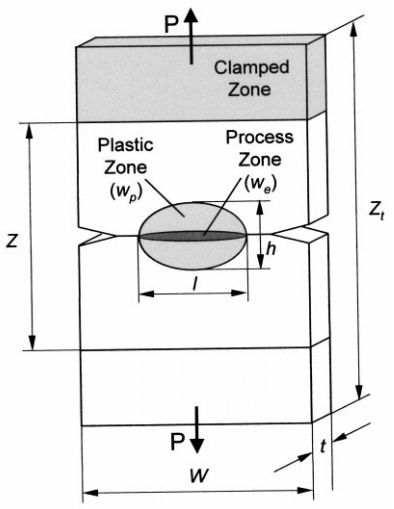

Fig. 1. DDEN-T specimen used for the Essential Work of Fracture tests. A schematic representation of the different zones is shown.

specimen thickness and β is a plastic zone shape dimensionless factor. The specific work of fracture is then:

$$w_f = W_f/lt = w_e + \beta w_p l \quad (2)$$

According to this equation, the plot of w_f as a function of l should be a linear relation, whose intercept with the Y-axis and slope would give w_e, and βw_p, respectively. Thus, the EWF method consists of testing specimens with different ligament lengths, measuring W_f for each (area under the force–displacement curve), plotting the w_f–l diagram and calculating the best-fit regression line. More details about the restrictions on the ligament length and its discussion, according to the European Structural Integrity Society (ESIS) EWF protocol [17] are given elsewhere [9] (and in the references therein). As the calculation of the w_p parameter is omitted in the last protocol, the 1993 version [18] has been used to calculate it, although a new shape-factor calculation is introduced in the present work.

2. Material

With the objective of studying simultaneously the materials and the possibilities of EWF as a means for toughness measurements, three commercial grade PPs with different ductility were chosen: one homopolymer (called H0) and two low-ethylene-content block copolymers (EPBC) or impact copolymers, with 5.5 and 12% ethylene (called C1 and C3, respectively), as determined by Fourier Transformed Infra Red (FTIR). The material was received in the form of pellets, and was cast-extruded to obtain 90 μm nominal thickness unoriented films, which were treated for 1 h in a fan-assisted oven at different annealing temperatures (T_a) between 80 and 150°C (measured to ±2°C). Then, the annealed films were conditioned at 23°C and 50% RH for 48 h, prior to testing. The nomenclature used refers to the material, followed by the annealing temperature (UA means unannealed).

3. Experimental

3.1. Differential scanning calorimetry (DSC)

A Perkin-Elmer Pyris1 thermal analysis system was used for heat flow measurements in order to study the smectic to monoclinic transition. The temperature and heat flow scales were calibrated using high purity indium and lead samples. About 8 mg of the specimens treated under various annealing conditions were studied at a heating rate of 10°C/min, from 40 to 200°C. The melting temperature of smectic and monoclinic phases, T_m^{sm} and T_m, respectively, were reported.

3.2. Wide-angle X-ray scattering (WAXS)

Wide-angle X-ray scattering patterns of H0 samples under all annealing conditions were recorded from samples that consisted of two 50 mm squares mounted on a Silice monocrystal. A Siemens D-500 diffractometer was used with Cu-K_α radiation, a 2θ range from 1.5 to 50°, a step size of 0.05° and a scan rate of 1°/min. From the scans, the degree of crystallinity (X_c) of the various samples was deduced by estimating the contribution of the crystalline and amorphous regions to the scattering pattern area [19]. Also, the average crystal thickness (L) was deduced using the Scherrer equation [20]:

$$L = \lambda/(D\cos\theta) \quad (3)$$

where L is the apparent crystal size (Å), λ is the wavelength used (Å), D is the half-height angular width (rad), and θ is the diffraction angle.

3.3. Tensile tests

Tensile tests were conducted on a universal testing machine (Adamel Lhomargy) equipped with a 100 N load cell, at 23 ± 1°C (RT) and crosshead speed of 10 mm/min. To increase the accuracy of the results, the dumb-bell specimens, tested according to ASTM D638-91, were individually measured for their thickness with an induction based coating measurer (precision of 1 μm). The yield stress (as the maximum stress) and the elastic modulus were calculated from the engineering stress–strain curves.

3.4. Fracture tests

The EWF tests were performed on the same machine as the tensile tests, at RT and a crosshead speed of 2 mm/min. Tests with specimens of the three materials were carried out, though in only three annealing conditions: UA, A120 and A140. Deeply double edge-notched samples (DDEN-T, Mode I) were prepared by cutting the sheets into rectangular coupons of total length $Z_t = 90$ mm (with a length between the grips of $Z = 60$ mm) and of width $W = 60$ mm (Fig. 1).

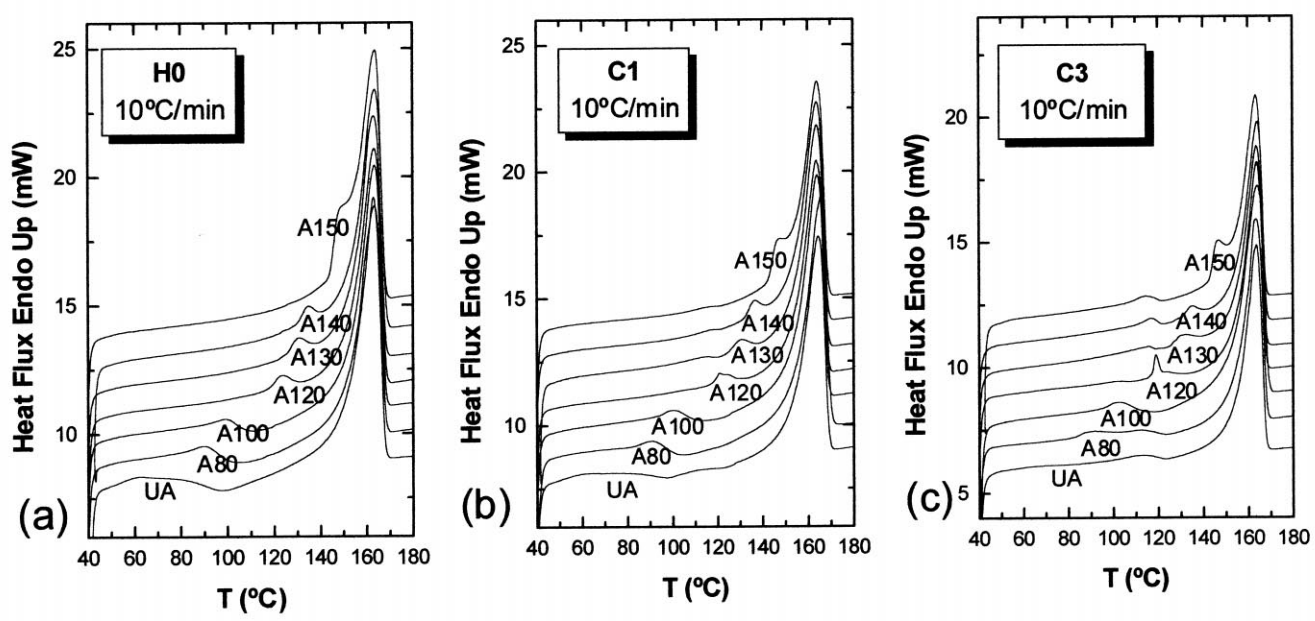

Fig. 2. Melting DSC curves of homopolymer and copolymers annealed at various temperatures, obtained at 10°C/min.

Initial notches were made perpendicularly to the tensile direction (which coincided with the extrusion direction) with a fresh razor blade, obtaining for each set at least 24 specimens with ligament lengths varying between 1 and 25 mm. The ligament lengths and the thickness were measured before the test using a travelling binocular lens microscope and the apparatus described above, respectively. The load vs displacement curves were recorded, and the absorbed energy calculated by computer integration of the loading curves.

4. Results and discussion

4.1. Annealing-induced phase transition

The DSC results in Fig. 2 show that there are clear differences between the curves when T_a is varied. Analysing the H0 sample response for simplicity (no additional melting peaks due to ethylene sequences are present in the homopolymer), it can be seen in Fig. 2(a) that there is an endotherm (T_m^{sm}) before the main melting peak (T_m). The value of T_m^{sm} varies gradually with the annealing temperature, while the main melting endotherm is found to have the maximum around $T_m = 163$°C, independent of the thermal history of the sample. The pre-melting peak is situated around T_a (see Table 1), thus indicating that there is a strong interrelation between both temperatures. For the unannealed sample, this peak is broader, with a maximum at about 60°C, and its temperature increases with the heat-treatment temperature. This fact is probably related to an increase in crystal thickness [21]. As has already been stated by other groups [1,2,13,20–23], this endotherm reveals the presence of the smectic metastable phase, and has been attributed to the melting of small monoclinic crystals formed during the original quenching process. These works show that, for the annealed samples, T_m^{sm} depends mainly on the annealing temperature, but also on the annealing time, generally reporting that the main effect is reached after about 1 h of thermal treatment. This annealing time (1 h) was chosen in the present work after some exploratory analysis that confirmed this fact. After the first endotherm, an exothermic peak shows that there is a re-ordering process that involves recrystallisation of the crystals just before melting in a more stable PP form. In fact, the difference in the melting enthalpy area of the recrystallisation exotherm compared to the monoclinic melting endotherm brought Alberola et al. [1] to suggest that the less stable microcrystallites progressively melt, while almost simultaneously, new crystallites, which are increasingly thicker and/or stable are formed, thus compensating the endothermic melting process by a re-ordering process involving energy dissipation.

The copolymers show an identical thermal response to the homopolymer (Fig. 2(b) and (c)), with the addition of a

Table 1
Influence of annealing on the microstructural and mechanical properties for H0

T_a (°C)	X_c	L (Å)	T_m^{sm} (°C)	σ_{max} (MPa)	E (MPa)
UA	0.36	24.7	60.5	20.32	1015
80	0.39	24.7	89.2	21.83	1039
100	0.43	92.3	98.5	24.66	1223
120	0.55	119.2	123.3	28.26	1565
130	0.58	119.2	130.3	29.46	1602
140	0.62	136.2	134.3	30.54	1644
150	0.65	159.9	147.9	33.36	1854

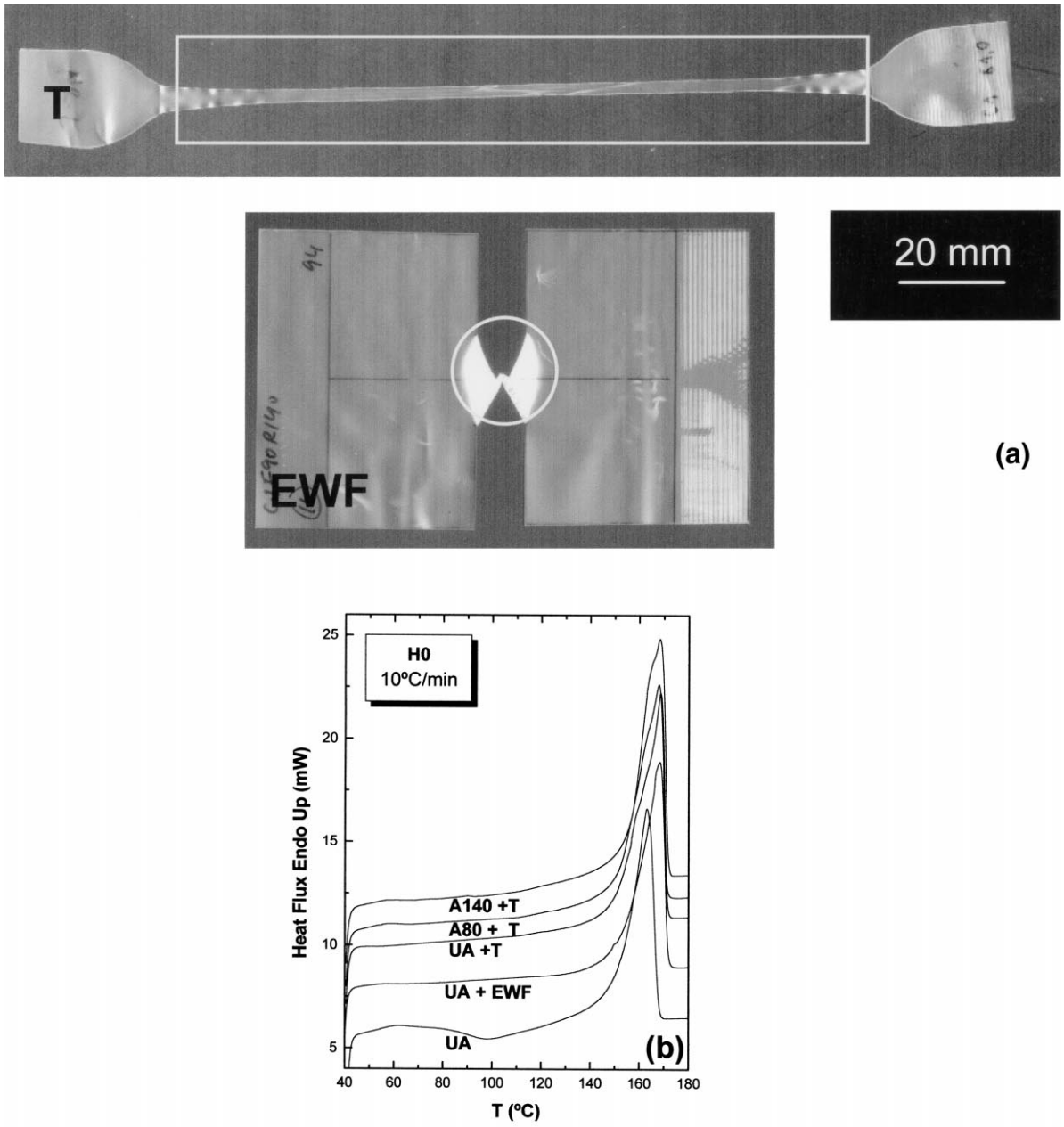

Fig. 3. (a) Tensile (T) and DDEN-T (EWF) samples after testing, showing the deformed region where the DSC samples were taken; (b) melting DSC curves for annealed and unannealed H0 films, taken in the deformed and undeformed regions of the samples shown in Fig. 3(a).

small endothermic peak at 115–120°C, which corresponds to the melting of the crystallites made of ethylene sequences. Such a peak is higher for C3, as the ethylene content of this material is about twice that of C1, and it can also be observed how this peak superposes to the smectic one for the C3A120 sample, as both signals occur at the same temperature.

Taking into account all these facts, the value of T_m^{sm} can be taken as a simple indication of the order perfection of the material (strongly related to the crystal size [21]) at different annealing conditions.

4.2. Strain-induced phase transition

According to a recent work [2], by applying plastic deformation to a quenched film the *sm*-PP → α-PP transformation is also induced, bringing a disorder–order transition. It is interesting to note that Karger-Kocsis [11] suggested that the phase transition from a less towards a more dense crystalline state may be a means for toughness improvement (commonly called Phase Transformation Toughening or PTT). In the case referred to, the transition that was occurring with applied strain was from the hexagonal and less

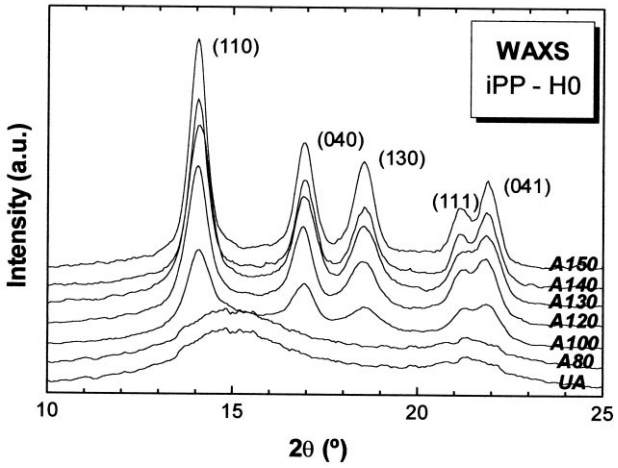

Fig. 4. WAXS patterns of H0 films with different annealing conditions.

dense β-PP form to the monoclinic and more compacted α-PP form, though the *sm*-PP is also less dense than α-PP.

In this work, various DSC samples of H0 were taken from the deformed part of tested tensile and fracture specimens (Fig. 3(a)), some of which had suffered a previous annealing process. The deformed part of the tensile specimens had reached a strain (ϵ) level of 300% (the tests were interrupted before the final fracture), roughly the same value of ϵ to that occurring in the sample extracted from the EWF specimens, though it is more difficult to estimate it due to the fact that ϵ can vary from one part to another in the plastic zone. The DSC curves in Fig. 3(b) indicate that the *sm*-PP peak disappears for the deformed specimens, suggesting that no trace of metastable phase remains after applying these strain levels. Moreover, all curves are very similar, independent of their thermal history before the plastic deformation. As explained by Seguela et al. [2], the reason for this transition is probably that the mechanical work brought about by the applied load helps the metastable crystals to transform into more stable α-PP crystals during the deformation process. On the other hand, the melting peak temperature of the strain induced α-PP phase increases about 6°C in relation to the undeformed sample, suggesting that the plastic yielding contributes in a better way to improve the perfection of all crystals, compared with the annealing-induced structure.

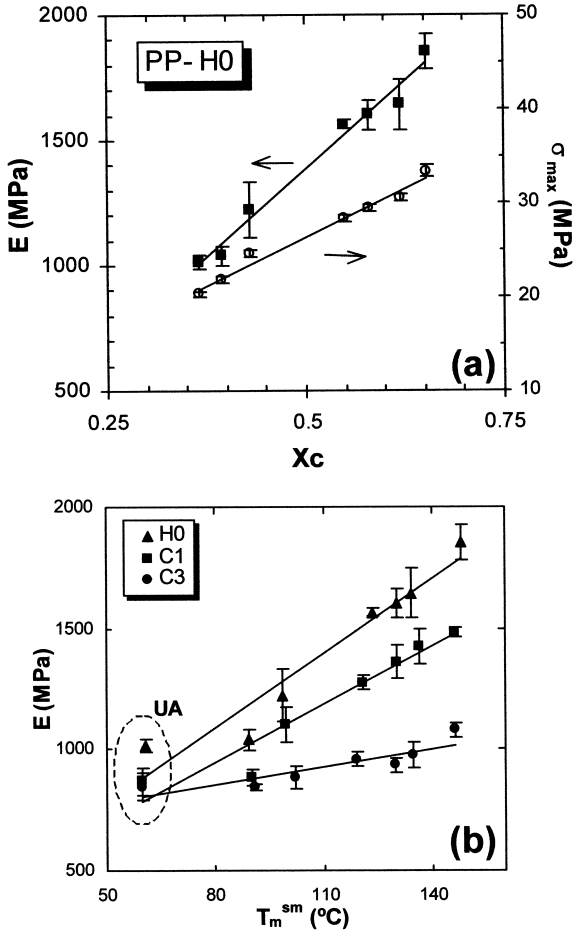

Fig. 5. (a) Evolution of the mechanical properties with the crystallintiy for the H0; (b) correlation of the elastic modulus with smectic phase melting temperature.

4.3. WAXS

The WAXS intensity profiles of H0 samples with various thermal treatments are shown in Fig. 4. They corroborate the DSC results, as the crystalline phase evolution from *sm*-PP to α-PP can be very well observed. The *sm*-PP structure (found in the UA and A80 samples) is revealed by the presence of a broad peak at about 15°, while the α-PP phase (which starts to appear for $T_a = 100$°C) gives a narrow peak localised at 14° (among other peaks at higher 2θ values, indexed in Fig. 4). Between the extreme cases (UA and A150), a wide range of intermediate states are found, which agrees well with the gradual increase in crystal perfection that could be followed by the DSC thermograms. These profiles have been used for calculating the crystal size and the crystallinity (Table 1). It can be observed that both parameters increase clearly with the annealing temperature, mainly at $T_a > 80$°C. WAXS is shown to be a good means to measure X_c, which is particularly interesting as it could not be calculated by analysing the DSC traces because the re-ordering process occurs during the temperature scan, thus modifying the enthalpy absorption that should correspond to the initial frozen structure.

4.4. Mechanical behaviour

The mechanical parameters reported, E and σ_{max} (Table 1), are highly improved with increasing T_a for H0, though the copolymers present similar variations. Such a result is doubtless related to the *sm*-PP phase evolution already commented on in previous sections, as it is well known that an improvement in crystal perfection, packing and size enhances the mechanical properties in semicrystalline polymers [1,2,24–26], due to better molecular cohesion of the α-PP compared to the *sm*-PP. If tensile properties are

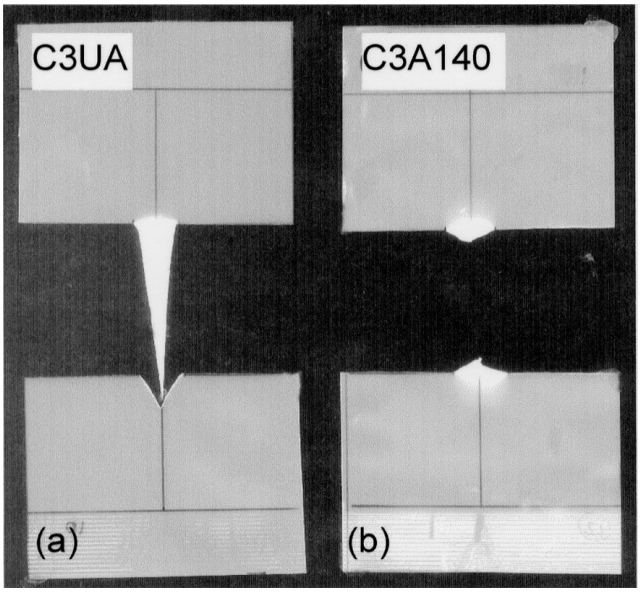

Fig. 6. Broken DDEN-T specimens of unannealed and annealed samples of C3.

correlated to the microstructural parameters calculated previously, one can find very good relations as shown in Fig. 5(a) and (b). It can also be observed that the improvement of the mechanical properties is rather similar for the three materials in the quenched state, and increasingly different as the monoclinic state is approached (detected by an increase in T_m^{sm}). This could indicate that the role of the ethylene blocks is increased when the crystalline perfection is improved, while this phase has little influence in the presence of the smectic form of iPP.

4.5. Fracture behaviour

The fracture of EWF samples was ductile and showed the typical behaviour of iPP, widely described in previous works [8,27], with a stable and ductile crack propagation as shown in Fig. 6(b). However, the C3UA set underwent an unusual propagation behaviour: in spite of starting to propagate perpendicular to the tensile direction, in all specimens of this set both cracks grew in a 60° direction from the notch plane (Fig. 6(a)), producing an intermediate state between tensile and fracture tests, as the extension to failure reached much higher values than are usually found in EWF tests. Thus, the use of the EWF procedure was discarded for this set, and the reasons for such behaviour are being studied in detail but will not be treated in the present work. However, it is to be noticed that similar problems with propagation have been found during our work with PP films when they were tested at higher temperatures than RT, which might reflect a limitation of the method. In a recent paper, Karger-Kocsis [28] also discusses this kind of phenomenon observed in rubber toughened PP with a skin-core morphology. It would seem that for high ductility conditions (*sm*-PP, high T, high rubber content), a strong blunting may render the normal propagation of the crack difficult or irregular.

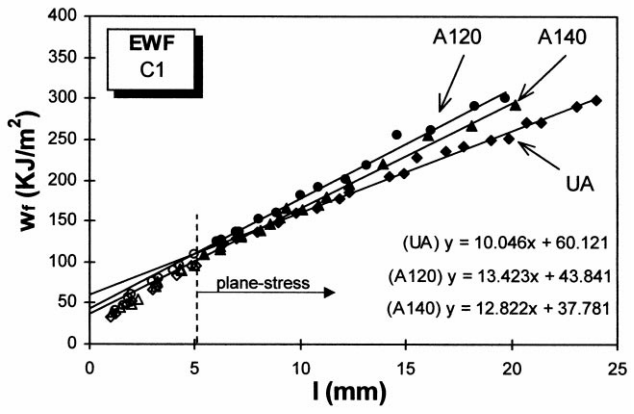

Fig. 7. Plot of specific work of fracture vs ligament length for the C1 films in three annealing conditions.

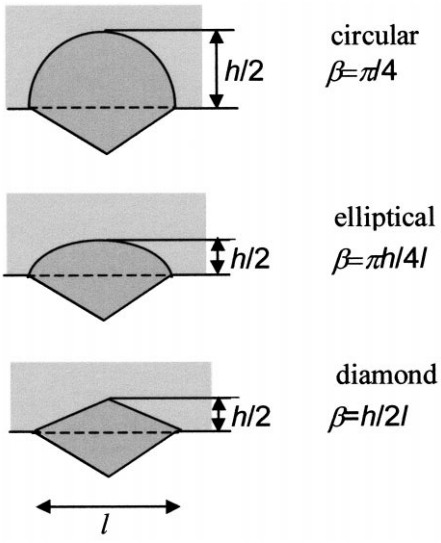

Fig. 8. Typical plastic zone shapes proposed in the ESIS EWF protocol of 1993.

As an example of the w_f vs l diagrams obtained, Fig. 7 shows the plots for C1UA, C1A120 and C1A140. Only the data with $l > 5$ mm were used for the calculation of the regression lines, because as has been widely discussed in other works [8,9] and in the references therein, and as is stated in the last EWF protocol version [17], the plane-stress fracture mode appears for $l > 5$ mm. Below this threshold, mixed-mode conditions prevail during the fracture process, giving lower fracture work values.The value of β (shape factor) was determined by using the relation between h (plastic zone height) and l, as recommended in the first EWF protocol version [18], which suggests three different possibilities for the plastic zone shape (circular, diamond and elliptical, shown in Fig. 8). Usually, this zone has an intermediate shape between elliptical and diamond, as can be seen in the figures reported in several works [29–33]. However, a new plastic zone shape that the authors think gives a better representation of the deformed region is used

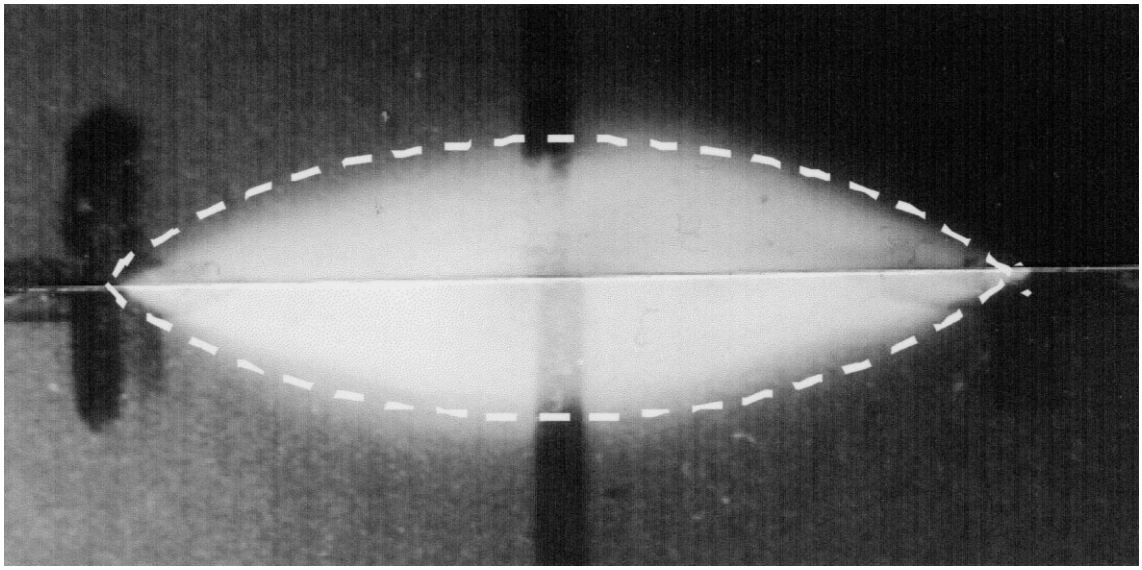

Fig. 9. Shape of the parabolic plastic zone proposed (the picture is the result of joining both sides of a C1 broken specimen with a strong stress-whitening in the deformed zone).

in the present work. This is a shape resulting from the intersection between two parabolas, giving an 'eye'-shaped region (Fig. 9), and that can be defined by the equation:

$$h = k \cdot \beta \cdot l, \tag{4}$$

with $k = 1.5$ (h is the height of the plastic zone, k is a constant that takes the values 2 and 1.27 for the diamond and ellipse cases, respectively). Thus, β can be determined as the slope of the h vs l plot regression line [18] divided by a factor of 1.5. Once β is found, w_p can be easily deduced from the slope of the regression lines of the w_f vs l diagrams.

Although w_p has been calculated by means of estimation of the plastic zone size, in this work the discussion and the comparisons between the materials are going to be treated in terms of βw_p concerning the plastic term of the fracture parameters. The reason is that βw_p is a global parameter that takes into consideration the whole plastic energy spent. It combines β, which is a material dependent plastic zone shape factor, with w_p, which is the material dependent specific energy absorption per unit volume. However, the calculation of w_p may be interesting in other cases, which justifies the interest in measuring this parameter with better accuracy.

Table 2
Influence of annealing on the EWF parameters calculated for H0, C1 and C3

T_a (°C)	Material	w_e (kJ/m^2)	βw_p (MJ/m^3)	β	w_p (MJ/m^3)
UA					
	H0	59.812	11.15	0.104	107.487
	C1	60.121	10.046	0.120	83.763
	C3	–	–	–	–
120					
	H0	62.026	12.913	0.066	196.845
	C1	43.841	13.423	0.117	114.726
	C3	37.819	9.1214	0.100	91.214
140					
	H0	47.513	15.543	0.069	225.479
	C1	37.781	12.822	0.161	79.475
	C3	28.321	8.9537	0.170	52.525

The analysis of the fracture results listed in Table 2 and summarised in Fig. 10 reveals that though it was shown that annealing produced a clear and gradual change in tensile properties, the effect on the toughness is more complex. At a first approach, the results show that the homopolymer (squares) shows almost in all cases higher w_e and βw_p values than the copolymers (triangles and circles), which indicates that an increase in the ethylene content of EPBC does not improve the toughness when these are tested at low strain rates and RT, where ductile failure prevails (further work is being done to find out if this tendency is inverted at high strain rates or at low temperature).

Moreover, it can be observed (Fig. 10) that the fracture values of the H0UA and C1UA samples are rather similar, thus indicating that in the smectic state the influence of the ethylene phase on the fracture properties is small (no data for the C3UA are available, as explained before). On the other hand, when the thermal treatment allows the re-ordering process *sm*-PP $\rightarrow$ α-PP to be carried out, the values of the fracture parameters become more different from one material to another. This agrees well with the analysis of the mechanical properties variation with annealing temperature (see Fig. 5(b)).

Taking into account the H0, one can observe that w_e goes through a maximum and decreases while βw_p increases as T_a is increased. This reflects the clearly different nature of the two energy dissipation parameters, and the fact that the

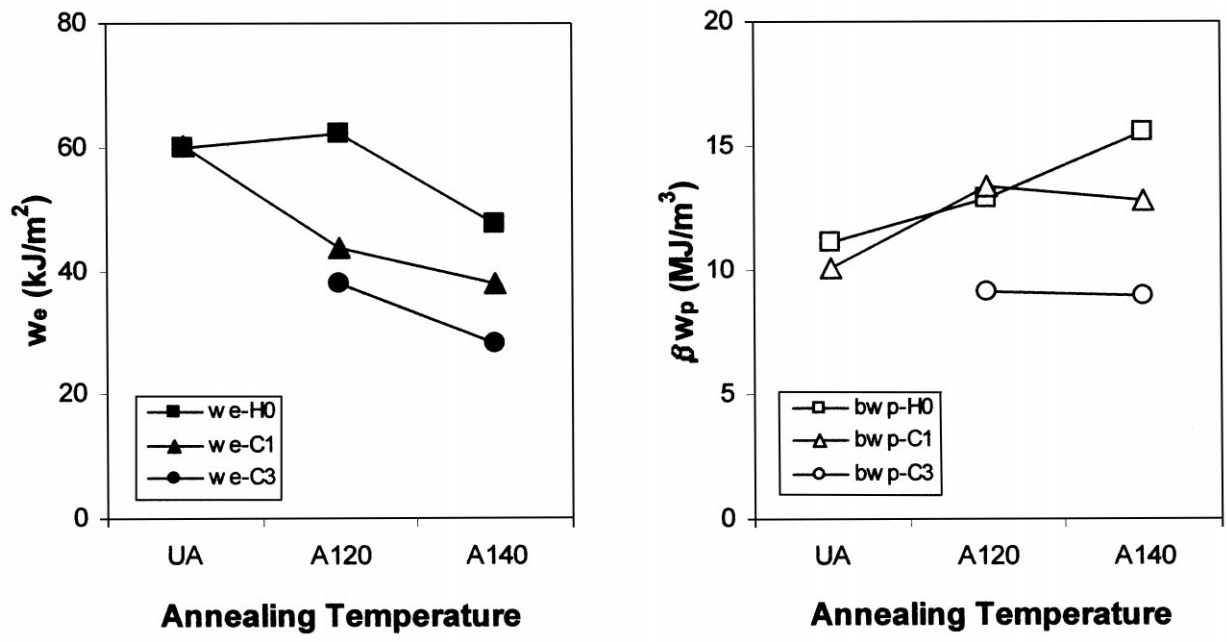

Fig. 10. Evolution of the EWF fracture parameters with annealing temperature for H0, C1 and C3.

whole fracture process can hardly be described by a single parameter, as has also been claimed in the literature [35]. It can also be seen that, for the copolymers, the essential work term decreases with an increase in T_a, and that the plastic work (βw_p) only increases until 120°C and stabilises at higher temperatures. Roughly, what Fig. 10 shows is that w_e (the value associated to the actual fracture process zone) decreases whereas βw_p increases as the annealing temperature (and therefore the crystal perfection) increases. This agrees fairly well with the results of Mouzakis et al. [34], who found that, for an elastomeric PP (ELPP), w_e increased and βw_p decreased with decreasing crystallinity. A possible explanation for this fact is given by Karger-Kocsis [35], who claims that the toughness dependence on the crystallinity relies on two facts: on the one hand, as the crystal perfection — crystallinity, molecular arrangement, lamellar size, etc. — grows, the toughness in the bulk crystals increases because destroying this structure implies a strong energy consumption; on the other hand, an increase in the crystal perfection can be obtained by reducing the number of tie molecules, which act as stress-transfer units between the crystalline zones. Thus, a crystallinity threshold may exist, and when it is overcome a decrease in toughness appears due to the lack of tie molecules. This hypothesis can reasonably be taken as the explanation for the fracture behaviour of the materials studied since, as has already been described, a change in the microstructure into a more crystalline state occurs. These considerations are reinforced by the observations of Alberola et al. [1] who claimed that a clear loss in the degree of entanglement between amorphous and crystalline phase occurred as the iPP quenched films were annealed. Considering that scenario, one can wonder why βw_p increases with X_c if the number of stress-transfer units would be decreasing. As has been stated, the two EWF parameters are related to different phenomena. On one hand, while w_e is the energy necessary to create two new surfaces, it is actually the work done to separate physically the material into two parts. On the other hand, βw_p includes a sum of plastic deformation mechanisms that occur around the fracture path (but out of it), and that may be affected differently from the toughness (w_e) by a decrease in the cohesion of the material. In fact, due to the high constraint in which this plastic strain is being produced, an increase in the stiffness (due to the increase in crystallinity and the subsequent growth of the mechanical properties) may be responsible for this increase in the plastic term.

Another interesting consideration in the case studied is the fact that a phase transformation occurs during the fracture deformation process, as described in a previous section. Recently, it was shown [11]that β-PP undergoes a mechanically-induced β-PP → α-PP transformation during fracture tests above T_g, and that concerning the EWF properties, w_e was the same for β- and α-PP, whereas the plastic term βw_p was three times higher for the β-PP. The reason that was given was that the change in the crystalline state towards a higher crystalline density is the key factor for improvement in fracture energy consumption. In our case, the *sm*-PP also has a lower density compared to α-PP (0.916 and 0.936) [36], though no increase in the plastic term is observed for the less dense phase material. On the contrary, an increase in w_e and an opposite trend in βw_p are found. This suggests that PTT does not imply necessarily an improvement of the plastic work. As presented in this work, it may produce an increase in the essential work term. Some differences can be explained by considering that *sm*-PP and α-PP are not two completely different microstructures as β-PP and α-PP are

but, though it is still a controversial matter, *sm*-PP is, in some manner, an intermediate form of iPP between amorphous and monoclinic.

5. Conclusions

It has been demonstrated that annealing PP and EPBC films has serious consequences on its microstructure, producing a gradual smectic to monoclinic phase transition as the temperature is increased above 80°C, and therefore an important gain in crystallinity and crystal size. The transition can also be promoted by strain deformation, obtaining more perfect crystals than by annealing (probably due to the orientation process).

The tensile properties are highly improved by the annealing induced microstructural changes, and can be very well correlated to crystallinity, crystal size and smectic phase melting temperature.

These changes in mechanical and fracture properties are more sensitive in the homopolymer than in the copolymers. It can be observed that, in the smectic state, these properties are similar for the three materials studied, thus seeming rather independent of the ethylene content in this iPP form. Thus, it can be concluded that the presence of the long-order phase seems to be more important with regard to the fracture properties than that of the ethylene sequences.

The improvement in crystal perfection produces a progressive loss in toughness (w_e), but an increase in the plastic work (βw_p). An explanation for these findings could come from a lack in stress-transfer between the ordered zones in the material by a simultaneous increase in the crystal perfection and decrease in the number of tie molecules, though no experimental data can definitively support this idea. However, a more complex scenario appears if one tries to find evidences of PTT, attributed to the *sm*-PP → α-PP transition that takes during the deformation. In that way, more work is being carried out to elucidate what are the actual causes of these variations in the fracture parameters. At least, one can claim that if PTT occurs, it does it in a different way than for β-PP.

As has already been stated recently [28], the results of this work reinforce the idea that, by varying one microstructural property, it is difficult to increase both fracture parameters at the same time, which implies that a compromise between them has to be made in relation to the properties desired for the material.

It has also been shown that it is difficult to characterise the fracture properties of ductile materials with a single parameter, because they represent different processes that occur simultaneously during fracture. In that way, the comparison between the toughness of different materials using the EWF procedure should take into account both essential and non-essential (including the plastic shape factor) terms.

A new plastic zone shape, with a parabolic geometry, is proposed for assessment of the plastic work in the EWF protocol, and may prove useful in the evaluation of w_p.

Acknowledgements

D. Ferrer-Balas is grateful to the CICYT for a predoctoral grant. The authors wish to thank Dr I. Iribarren for his helpful discussions, and the supplier of the materials, Targor Group.

References

[1] O'Kane WJ, Young RJ, Ryan J, Bras W, Derbyshire GE, Mant GR. Polymer 1994;35:1352.
[2] Seguela R, Staniek E, Escaig B, Fillon B. J Appl Polym Sci 1999;71:1873.
[3] Alberola N, Fugier M, Petit D, Fillon B. J Mater Sci 1995;30:860.
[4] Frontini PM, Fave A. J Mater Sci 1995;30:2446.
[5] Greco R, Ragosta G. J Mater Sci 1988;23:4171.
[6] Ito JI, Mitani K, Mizutani Y. J Appl Polym Sci 1992;46:1221.
[7] Wu J, Mai YW. Polym Engng Sci 1996;36:2275.
[8] Maspoch MLl, Ferrer D, Gordillo A, Santana OO, Martinez AB. J Appl Polym Sci 1999;73:177.
[9] Maspoch MLl, Hénault V, Ferrer-Balas D, Velasco JI, Santana OO. Polym Test 2000;19:559.
[10] Chan WYF, Williams JG. Polymer 1994;35:1666.
[11] Karger-Kocsis J. Polym Engng Sci 1996;36:203.
[12] Natta G, Peraldo M, Corradini P. Rand Accad Naz Lincei 1959;26:14.
[13] Vittoria V. J Macromol Sci, Phys 1989;B28:489.
[14] Zanetti R, Celotti G, Fichera A, Francesconi R. Makromol Chem 1969;128:137.
[15] Cotterell B, Reddel JK, Int. J Fract 1977;13:267.
[16] Broberg KB, Int. J Fract 1968;4:11.
[17] Clutton E. Testing protocol for Essential Work of Fracture, ESIS-TC4, 1997.
[18] Gray A. Testing protocol for Essential Work of Fracture, ESIS-TC4, 1993.
[19] Young RJ, Lovell PA. Introduction to polymers. 2. London: Chapman and Hall, 1991.
[20] Poussin L, Bertin YA, Parisot J, Brassy C. Polymer 1998;18:4261.
[21] Jourdan C, Cavaille JY, Perez J. J Polym Sci, Polym Phys 1980;18:493.
[22] O'Kane WJ, Young RJ, Ryan AJ. J. Macromol Sci, Phys 1995;B34:427.
[23] Romano G, Russo R, Vittoria V. J Macromol Sci, Phys 1998;B37:841.
[24] Wills AJ, Capaccio G, Ward IM. J Polym Sci Polym Phys 1980;18:493.
[25] Gesovich D, Geil P. Polym Engng Sci 1968;8:202.
[26] Rolando RJ, Krueger WL, Morris HW. Polym Mater Sci Engng 1985;52:76.
[27] Ferrer-Balas D, Maspoch ML, Martinez AB, Santana OO. Polym Bull 1999;42:101.
[28] Karger-Kocsis J, editor. Prodeedings of the 2nd ESIS TC4 conference on polymers and composites. Elsevier Science, 1999.
[29] Mouzakis DE, Stricker F, Mülhaupt R, Karger-Kocsis J. J Mater Sci 1998;33:2551.
[30] Hashemi S. Polym Engng Sci 1997;37:912.
[31] Levita G, Parisi L, Marchetti A. J Mater Sci 1994;29:4545.
[32] Karger-Kocsis J, Czigány T, Moskala EJ. Polymer 1998;39:3939.
[33] Karger-Kocsis J, Czigány T. Polymer 1996;37:2433.
[34] Mouzakis DE, Gahleitner M, Karger-Kocsis J. J Appl Polym Sci 1998;70:873.
[35] Karger-Kocsis J. In: Cunha AM, Fakirov S, editors. Structure development during polymer processing, NATO-ASI Series. Dordrecht: Kluwer Academic, 2000.
[36] Vittoria V. J Mater Sci 1992;27:4350.